Bose-Einstein condensation of magnons in quantum magnets with spin-orbit coupling in a Zeeman field

Fadi Sun[1,2] and Jinwu Ye[1,2,3]

[1]*School of Sciences, Great Bay University, Dongguan 523000, Guangdong, China*

[2]*Institute for Theoretical Sciences, Westlake University, Hangzhou 310024, Zhejiang, China*

[3]*Department of Physics and Astronomy, Mississippi State University, Mississippi State, Mississippi 39762, USA*

(Received 9 June 2021; revised 11 November 2022; accepted 24 April 2023; published 12 May 2023)

We study the response of a quantum magnet with spin-orbit coupling (SOC) to a Zeeman field by constructing effective actions and performing renormalization group (RG) analysis. There are several novel classes of quantum phase transitions at a low h_{c1} and an upper critical field h_{c2} driven by magnon condensations at commensurate (C) or incommensurate (IC) momenta $0 < k_0 < \pi$. The intermediate IC-skyrmion crystal (IC-SkX) phase is controlled by a line of fixed points in the RG flows labeled by k_0. We derive the relations between the quantum spin and the order parameters of the effective actions which determine the spin-orbital structures of the IC-SkX phase. We also analyze the operator contents near h_{c1} and h_{c2} which determine the exotic excitation spectra inside the IC-SkX. The intrinsic differences between the magnon condensations at the C and IC momenta are explored. The two critical fields $h_{c1} < h_{c2}$ and the intermediate IC-SkX phase could be a generic feature to any quantum magnets with SOC in a Zeeman field. Experimental implications to some materials or cold atom systems with SOC in a Zeeman field are presented.

DOI: 10.1103/PhysRevB.107.184425

I. INTRODUCTION

In 1938, the Bose-Einstein condensation (BEC) was first observed in the superfluid state of ^{4}He which is a strongly interacting system [1]. In 1995, it was also observed in a dilute gas of alkali atoms which is a weakly interacting system [2,3]. In the BEC, the global $U(1)_c$ symmetry corresponding to the boson number conservation is spontaneously broken, which leads to the Goldstone mode with a linear dispersion. It was known that the magnon condensation tuned by a Zeeman field in a quantum magnet [4–10] can be mapped to the BEC with the spin $U(1)_s$ symmetry mimicking the charge $U(1)_c$ symmetry of the bosons. Here, inspired by many recent experimental studies on the response to a Zeeman field of some chiral magnets [11] and 4*d* or 5*d* Kitaev materials [12,13] with strong spin-orbit coupling (SOC), we study the magnon condensation in a quantum magnet with SOC in a Zeeman field and find it leads to dramatically new phenomena outlined in the abstract and Fig. 1.

The system is the interacting spinor bosons at integer fillings hopping in a square lattice in the presence of non-Abelian gauge fields studied in [14]. In the strong-coupling limit, it leads to the spin $S = N/2$ rotated ferromagnetic Heisenberg model (RFHM), which is a new class of quantum spin models to describe quantum magnetisms in cold atom systems or some materials with strong SOC. There is an exact $U(1)_{\rm soc}$ symmetry along the anisotropic line ($\alpha = \pi/2, 0 < \beta < \pi/2$) of the 2-dimensional SOC. Along the line, we identified a new spin-orbital entangled commensurate ground state: the Y-x state. It supports not only commensurate magnons (C_0, C_π), but also a new gapped elementary excitation: the incommensurate (IC) magnon. The existence of the C-IC above a commensurate phase is a salient feature of the RFHM. They indicate the short-ranged incommensurate order embedded in a long-range ordered commensurate ground state. The IC magnons may become the seeds to drive possible new classes of quantum C-IC transitions under various external probes. In [15], by performing the microscopic spin-wave expansion (SWE), we explored the effects of an external longitudinal Zeeman field H applied to the RFHM Eq. (1) along the anisotropic SOC line which keeps the $U(1)_{\rm soc}$ symmetry. However, the microscopic SWE approach used in [15] is essentially a semiclassical approach. It may not apply to a small quantum spin S in real materials, and will also break down near all the quantum phase transitions in Fig. 1. A completely independent symmetry-based phenomenological effective action is needed to study the nature of these novel quantum phase transitions.

In this work, starting from the general symmetry principle, we construct various effective actions, then perform renormalization group (RG) flows and carefully analyze the physically accessible initial conditions to study all the quantum phase transitions in Fig. 1. We also identify the relations between the quantum spins in a lattice and the order parameters in the effective actions, which are needed to identify the quantum spin-orbital orders of the phases. When away from the quantum critical points, we recover all these quantum phases and their excitations discovered by the microscopic calculations in [14,15]. Most importantly, we explore the nature of all the quantum phase transitions, and therefore provide deep insights into the global phase diagram in Fig. 1. The transition from the Z-x phase to the incommensurate skyrmion crystal (IC-SkX) phase at $h = h_{c1}$ is in the same universality class as the $z = 2$ superfluid (SF)–Mott transition [7,9]. In

 ©2023 American Physical Society

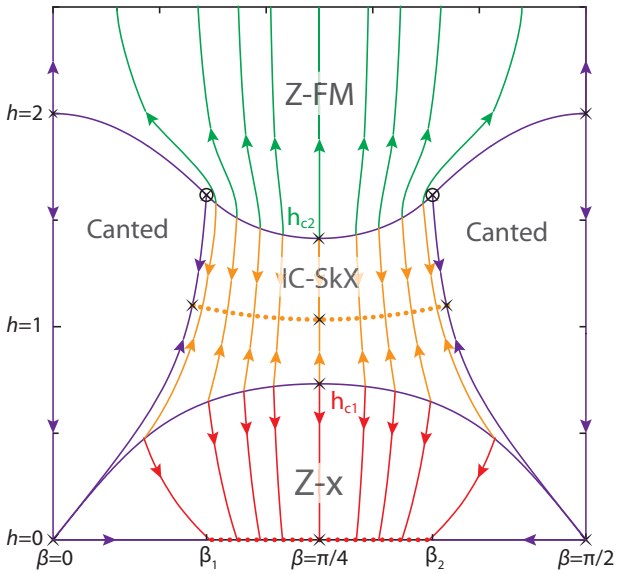

FIG. 1. Renormalization group (RG) flow of Eq. (1) which explores many new features of magnetic systems with SOC. Z-FM is a ferromagnet along the Zeeman field, IC-SkX is the incommensurate skyrmion crystal, and Z-x is the ferromagnet alternating along the x bond. There is a line of unstable fixed (or QPT) points labeled by the BEC condensation C or IC momentum k_0 in Eq. (2) and in Eq. (10) near h_{c1} and h_{c2}, respectively. There is also a line of stable fixed points labeled by the $0 \leqslant k_0 \leqslant \pi$ inside the IC-SkX phase. The RG flows just follow the constant contour line of k_0. The new universality classes of all these QPTs and the corresponding operator contents at or away from the two mirror symmetric points are analyzed in the text.

addition to the well-known type-I dangerously irrelevant operator (DIO) [7,9,16], there is also a new type-II DIO [17] which leads to one exotic Goldstone mode inside the IC-SkX phase near h_{c1}. At the mirror symmetry point $\beta = \pi/4$, the type-II DIO is absent; the exotic Goldstone mode recovers to the conventional one. The quantum phase transition (QPT) from the Z-FM to the IC-SkX at $h = h_{c1}$ is described by a novel two component effective action with the dynamic exponent $z = 2$ and a $U(1)_{\rm soc} \times U(1)_{ic}$ symmetry where the extra $U(1)_{ic}$ symmetry comes from the condensations of the magnons at the two IC momenta. It was spontaneously broken down to its diagonal $[U(1)_{\rm soc} \times U(1)_{ic}]_D$ leading one Goldstone mode inside the IC-SkX phase. By performing renormalization group flow analysis, we find it is a novel universality class with new operator contents. In addition to two type-I DIOs, there are also two type-II DIOs which lead to one exotic gapless Goldstone mode and one gapped exotic roton mode inside the IC-SkX phase near h_{c2}. At the mirror symmetry point, the two type-II DIOs are absent, and the exotic Goldstone and roton mode recover to conventional ones; a quartic umklapp term breaks the extra $U(1)_{ic}$ symmetry explicitly to Z_4 and becomes the third type-I DIO and plays important roles. The RG analysis on the effects of this umklapp term is performed. These results may shed considerable light on the experimental findings, especially the nature of the intermediate phases of some materials with strong SOC such as the chiral magnets and the Kitaev materials in a Zeeman field. Some perspectives are outlined.

Here, we focus on the RFHM along the line ($\alpha = \pi/2, 0 < \beta < \pi/2$) in the Zeeman field along the longitudinal y direction [15] (see also Appendix A). After rotating the spin Y axis to Z axis, it can be written as [18]

$$\begin{aligned}\mathcal{H} = & -J\sum_i \Big[\frac{1}{2}(S_i^+ S_{i+x}^+ + S_i^- S_{i+x}^-) - S_i^z S_{i+x}^z \\ & + \frac{1}{2}(e^{i2\beta} S_i^+ S_{i+y}^- + e^{-i2\beta} S_i^- S_{i+y}^+) + S_i^z S_{i+y}^z\Big] \\ & - H\sum_i S_i^z, \end{aligned} \tag{1}$$

where $J > 0$ and the Zeeman field H is along the z direction after the global rotation.

As shown in [14], Eq. (1) at $H = 0$ has the translational symmetry, the time-reversal symmetry $\mathcal{T}$, and the three spin-orbital coupled Z_2 symmetries $\mathcal{P}_x, \mathcal{P}_y, \mathcal{P}_z$. Most importantly, it also owns a hidden spin-orbital coupled $U(1)_{\rm soc}$ symmetry generated by $U_1(\phi) = e^{i\phi\sum_i (-1)^x S_i^z}$. The H breaks the $\mathcal{T}, \mathcal{P}_x, \mathcal{P}_y$ symmetries, but still keeps the translation, $\mathcal{P}_z$, the combinations $\mathcal{T}\mathcal{P}_x$, $\mathcal{T}\mathcal{P}_y$, and the hidden $U(1)_{\rm soc}$ symmetry. Under the mirror transformation $\mathcal{T}M$, where $\mathcal{M} = R(\hat{x}, \pi)R(\hat{z}, i_y\pi)$, it maps $(\beta, h) \to (\pi/2 - \beta, h)$. So one only needs to focus on the left half of Fig. 1. The mirror center $\beta = \pi/4$ respects the mirror symmetry. In the following, we will take $2SJ$ as the energy unit.

II. QUANTUM PHASE TRANSITION AT THE LOWER CRITICAL FIELD h_{c1}

The spin wave expansion (SWE) in the Z-x state below h_{c1} was performed in [15]. Dropping the higher branch $\alpha_{\mathbf{k}}$ in Eq. (A7), it is the $\beta_{\mathbf{k}}$ magnon condensation at $\mathbf{K}_0 = (0, k_0)$ which leads to the QPT from the Z-x state to the IC-SkX at h_{c1} in the whole range of $0 < \beta < \pi/2$:

$$\beta_{\mathbf{k}} = \psi\delta_{\mathbf{k},\mathbf{K}_0}, \quad \alpha_{\mathbf{k}} = 0, \tag{2}$$

where $\mathbf{K}_0 = (0, k_0)$ and ψ is a complex order parameter.

One must use the unitary transformation Eq. (A6) to establish the connection between the transverse quantum spin on the lattice and the order parameter in the continuum limit:

$$S_{A,i}^+ = \sqrt{2S}a_i = c\psi e^{ik_0 i_y}, \quad S_{B,j}^- = \sqrt{2S}b_j = s\psi e^{ik_0 j_y}, \tag{3}$$

where $c = c_{\mathbf{K}_0}$ and $s = s_{\mathbf{K}_0}$ are evaluated at $\mathbf{K}_0 = (0, k_0)$.

The Z-x state spontaneously breaks the translation along the x direction by one lattice site to two lattice sites, i.e., $\mathcal{T}_x \to (\mathcal{T}_x)^2$, but still keeps all the other symmetries of the Hamiltonian listed below Eq. (1). After incorporating this fact, one can study how ψ transforms under the symmetries of the Hamiltonian, especially under $\mathcal{T}_y$ as $\psi \to e^{ik_0}\psi$, $U(1)_{\rm soc}$ as $\psi \to e^{i\phi_0}\psi$. At the mirror symmetry point $\beta = \pi/4$, under $\mathcal{T}\mathcal{M}$ as $\psi \to -\psi^*$. The symmetry analysis suggests the following effective action in the continuum limit with the dynamic exponent $z = 2$,

$$\begin{aligned}\mathcal{L}_{h_{c1}} = & \psi^*\partial_\tau\psi + v_x^2|\partial_x\psi|^2 + v_y^2|\partial_y\psi|^2 - \mu|\psi|^2 + U|\psi|^4 \\ & + iV|\psi|^2\psi^*\partial_y\psi + \cdots, \end{aligned} \tag{4}$$

where $\cdots$ includes terms such as $i\psi^*\partial_y^3\psi$ and many other terms which are subleading in the RG sense [19]. Our microscopic calculation shows that $\mu = h - h_{c1}$ which tunes the QPT, $U > 0$, $V \propto \sin(2k_0)$ vanishes at $\beta = \pi/4$ dictated by the mirror symmetry. In fact, its symmetry-breaking pattern [20] and associated Goldstone mode are identical to Eq. (13), to be discussed in Sec. III.

When $h < h_{c1}$, $\mu < 0$, it is in the Z-x state with $\langle\psi\rangle = 0$. Expanding the effective action up to second order in ψ leads to the gapped excitation spectrum $\omega_{\mathbf{k}} = -\mu + v_x^2k_x^2 + v_y^2k_y^2$ which matches the results achieved by the microscopic SWE calculation in [15].

When $h > h_{c1}$, $\mu > 0$, it is in the IC-SkX state with $\langle\psi\rangle = \sqrt{\rho_0}e^{i\phi_0}$ where $\rho_0 = \sqrt{\mu/2U}$ and ϕ_0 is a arbitrary angle due to $U(1)_{\rm soc}$ symmetry. Plugging the mean field solution into Eq. (3), one obtain the spin-orbital order of the IC-SkX phase above h_{c1}:

$$\langle S_i^+\rangle = (\sqrt{\rho_0}/2)[c + s + (-1)^{i_x}(c - s)]e^{(-1)^{i_x}i(k_0i_y+\phi_0)}, \quad (5)$$

where $\langle S_i^z\rangle$ can be fixed by the constraint $|\mathbf{S}_i|^2 = S^2$. It has a nonvanishing skyrmion density $Q_{ijk} = \mathbf{S}_i \cdot (\mathbf{S}_j \times \mathbf{S}_k)$, where i, j, k are three neighboring lattice sites in a square lattice. Well inside the IC-SkX state, one can also extract its exotic Goldstone mode due to the $U(1)_{\rm soc}$ symmetry breaking:

$$\omega_{\mathbf{k}} = \sqrt{4U\rho_0\left(v_x^2k_x^2 + v_y^2k_y^2\right)} - V\rho_0k_y, \quad (6)$$

which recovers the conventional Goldstone mode at the mirror symmetry point $\beta = \pi/4$ where $V = 0$.

In the following, we use the Wilsonian momentum shell method to derive the RG flow near h_{c1} and h_{c2} at or away from the mirror symmetric point in Fig. 1. This method is the quickest one to achieve the RG flow at one-loop order. However, it is not practical when there is a gauge field, because it is very difficult to keep gauge invariance even at one-loop order [21]. It cannot be pushed into two loops either which can only be achieved by the Field theory method. Fortunately, one-loop order is enough to capture the physics in the present context. We first study the single-component case near h_{c1} to set up the scheme and notations, then investigate the more interesting two component cases near h_{c2}.

A. RG and operator contents at the mirror symmetric point

The effective action describing the magnon BEC in the presence of SOC near $h = h_{c1}$ at the mirror symmetric point $\beta = \pi/4$ in Fig. 1 is

$$\mathcal{S}_{h_{c1}} = \int d\tau d^dr\Big[\psi^*(r,\tau)\partial_\tau\psi(r,\tau) + \frac{\hbar^2}{2m}|\nabla\psi(r,\tau)|^2 - \mu|\psi(r,\tau)|^2 + u|\psi(r,\tau)|^4 + \cdots\Big], \quad (7)$$

where ψ is the complex scalar field. After adding back the type-II dangerously irrelevant operator (DIO) V in Eq. (4), it describes the QPT near h_{c1} away from the mirror symmetric point in Fig. 1. As shown in Eq. (B2) in the Appendix B, it also precisely describes the magnon BEC of the AFM in a uniform Zeeman field.

The major simplification of $z = 2$ over the relativistic case $z = 1$ is that when performing RG in the $z = 2$ theory, one must separate the frequency ω from the momentum $\vec{k}$, then the frequency integral $\int \frac{d\omega}{2\pi}$ will kill many Feymann diagrams which will otherwise make a contribution in a relativistic quantum field theory. Figure 2(a) is the only surviving diagram. Similar simplifications also apply to the two-component cases to be discussed in Secs. III and IV.

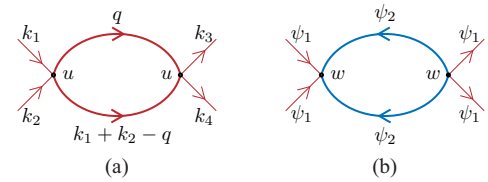

FIG. 2. The renormalization of the self-interaction u. The 3-momentum $k = (\vec{k}, \omega)$ is indicated in (a), and the red line and the blue line in (b) denote ψ_1 and ψ_2, respectively. The internal line is on the 2-momentum shell $\Lambda e^{-\delta l} < q < \Lambda$. (a) Due to u^2, (b) due to w^2.

The Wilsonian RG flow equation at one loop is given by Fig. 2(a):

$$\partial_l\mu = 2\mu,$$
$$\partial_l u = \epsilon u - cu^2, \quad (8)$$

where $\epsilon = 2 - d$ and $c = K_d\Lambda^{d-2}2m/\hbar$ with $K_d = S_d/(2\pi)^d = 2/[(4\pi)^{d/2}\Gamma(d/2)]$. In fact, we expect that Eq. (8) is exact to any loop order due to the exact $U(1)_{\rm soc}$ symmetry and $z = 2$. Our field theory RG analysis [21] on u confirms this expectation up to two loops.

In the present context of Fig. 1, u is marginally irrelevant near h_{c1}, but becomes relevant below the line of fixed points inside the IC-SkX phase in Fig. 1. Equation (8) has been extended to a finite temperature in [7]. The type-I DIO u leads to the logarithmic violations of scalings [7] to the conserved density $n = |\psi|^2$. Then using the relation between the quantum spin and the order parameter in Eq. (3), one can determine the logarithmic violations of scalings to various quantum spin correlation functions.

At the mirror symmetry point $\beta = \pi/4$, $V = 0$, so the effective action Eq. (4) is in the same universality class [22] as the $z = 2$ zero density SF-Mott transition where the interaction U term is marginally and dangerously irrelevant at the up-critical dimension $d_u = 2$. It determines the nature of the symmetry-breaking ground state and also leads to the logarithmic violation of scalings [7] to all the physical quantities at a finite temperature.

B. RG and operator contents away from the mirror symmetric point

When away from the mirror symmetry point, the V term in Eq. (4) moves in. Simple power counting shows that it is irrelevant near the SF-Mott QPT. However, inside the IC-SkX phase, as shown in Eq. (6), it modifies the spectrum of the Goldstone mode by an extra linear term, so it plays a crucial role inside the phase. We call this new type of DIO as type II [17], while the known one such as U as type I [7,9,16]. So there are one type-I DIO u and one type-II DIO V below the line of stable fixed points inside the IC-SkX (Fig. 1).

Away from the mirror symmetry point, one needs to add back the type-II dangerously irrelevant operator (DIO) V in Eq. (4), just by simple power counting, one finds at $d = 2$:

$$\partial_l V = -V, \tag{9}$$

which is clearly irrelevant near h_{c1}, but it changes the Goldstone mode into the exotic form inside the IC-SkX phase. So it becomes marginal below the line of fixed points inside the IC-SkX phase in Fig. 1. As shown below Eq. (4), the microscopic calculation finds $V \sim \sin(2k_0)$ which is indeed exactly marginal along the RG flow in Fig. 1 until hitting the line of fixed points labeled by k_0 inside the IC-SkX phase.

So we conclude that away from the mirror symmetry point, the operator content is one type-I DIO u and one type-II DIO V. At the mirror symmetry point, the operator content is one type-I DIO, no type-II DIO.

In Fig. 1, there are also two trivial lines of fixed points at $h = 0$ and $h = \infty$ which correspond to the Z-x state and FM state, respectively. Even it is just the same ground state, the line of fixed points characterized by $0 \leqslant k_0 \leqslant \pi$ still has clear physical meanings: it indicates the minima position of the IC magnons above the ground state. Of course, the Z-x state is an exact ground state, so it does not contain the IC magnons at $T = 0$. However, the lowest excitation is the IC magnons. The FM ground state contains the quantum fluctuations from the IC magnons even at $T = 0$. So it is justified to use k_0 to distinguish "different kinds" of the Z-x state at $h = 0$ and "different kinds" of FM at $h = \infty$ in Fig. 1. These could also be one the salient features of incommensurability due to SOC.

III. QUANTUM PHASE TRANSITION AT THE UPPER CRITICAL FIELD h_{c2}, THE INCOMMENSURATE CASE

The SWE in the FM state above h_{c2} was also performed in [15]. It is the $\alpha_{\mathbf{k}}$ magnon condensation in Eq. (A13) which leads to the QPT from the FM state to the IC-SkX at h_{c2} in the middle range $\beta_1 < \beta < \beta_2$ [23]:

$$\alpha_{\mathbf{k}} = \psi_1 \delta_{\mathbf{k},\mathbf{K}_1} + \psi_2 \delta_{\mathbf{k},\mathbf{K}_2}, \tag{10}$$

where $\mathbf{K}_1 = (0, k_0)$, $\mathbf{K}_2 = (\pi, k_0)$, and ψ_1, ψ_2 are the two complex order parameters.

One must use the Bogoliubov transformation Eq. (A12) to establish the connection between the transverse quantum spin and the two complex order parameters:

$$S_i^+ \propto u[\psi_1 + (-1)^{i_x}\psi_2]e^{ik_0 i_y} + v[\psi_1^* - (-1)^{i_x}\psi_2^*]e^{-ik_0 i_y}, \tag{11}$$

where $u = u_{\mathbf{K}_1} = u_{\mathbf{K}_2}$ and $v = v_{\mathbf{K}_1} = -v_{\mathbf{K}_2}$.

Because the Z-x state breaks no symmetry of the Hamiltonian, one can study how ψ_1 and ψ_2 transform under the symmetries of the Hamiltonian listed below Eq. (1), especially under $\mathcal{T}_y$ as $(\psi_1, \psi_2) \to (e^{ik_0}\psi_1, e^{ik_0}\psi_2)$, under $U(1)_{\text{soc}}$ as $(\psi_1, \psi_2) \to (\psi_1 \cos\phi + i\psi_2 \sin\phi, \psi_2 \cos\phi + i\psi_1 \sin\phi)$, and at the mirror symmetry point $\beta = \pi/4$, under $\mathcal{TM}$ as $(\psi_1, \psi_2) \to (-\psi_1^*, -\psi_2^*)$.

In fact, as suggested by Eq. (11), the physics may become more transparent in the new basis $\psi_\pm = (\psi_1 \pm \psi_2)/\sqrt{2}$. Under the whole family of $\mathcal{T}_y^n$, $n = 1, 2, 3, \cdots$, $(\psi_+, \psi_-) \to (e^{ik_0 n}\psi_+, e^{ik_0 n}\psi_-)$. When k_0/π is an irrational number, $\theta_0 = k_0 n$ becomes a continuous variable leading to a new emergent $U(1)_{ic}$ symmetry. Under $U(1)_{\text{soc}}$, $(\psi_+, \psi_-) \to (e^{i\phi_0}\psi_+, e^{-i\phi_0}\psi_-)$. The symmetry analysis implies the effective action

$$\begin{aligned}\mathcal{L}_{h_{c2}} = &\sum_{\alpha=\pm}\left(\psi_\alpha^*\partial_\tau\psi_\alpha + v_x^2|\partial_x\psi_\alpha|^2 + v_y^2|\partial_y\psi_\alpha|^2 - \mu|\psi_\alpha|^2\right)\\ &+ U(|\psi_+|^2 + |\psi_-|^2)^2 - A(|\psi_+|^2 - |\psi_-|^2)^2 + \cdots\\ &+ iV_1(|\psi_+|^2 + |\psi_-|^2)(\psi_+^*\partial_y\psi_+ + \psi_-^*\partial_y\psi_-)\\ &+ iV_2(|\psi_+|^2 - |\psi_-|^2)(\psi_+\partial_y\psi_+^* - \psi_-^*\partial_y\psi_-),\end{aligned} \tag{12}$$

which enjoys a $U(1)_{\text{soc}} \times U(1)_{ic}$ symmetry when k_0/π is an irrational number. Our microscopic calculation shows that $\mu = h_{c2} - h$, $U = h(u^2 + v^2)^2 + 2(1 + h) > A = (4 + h) > 0$. Furthermore, $V_1, V_2 \propto \sin(2k_0)$, both of which vanish at $\beta = \pi/4$ dictated by the mirror symmetry.

When $\mu < 0$, it is in the Z-FM phase with $\langle\psi_1\rangle = \langle\psi_2\rangle = 0$. Expanding the effective action up to the second order in ψ_α leads to two degenerate gapped modes $\omega_{1,2} = -\mu + v_x^2k_x^2 + v_y^2k_y^2$ which matches the result achieved by SWE in [15].

When $\mu > 0$, it is in the IC-SkX phase with $\langle\psi_1\rangle = \pm\langle\psi_2\rangle = \sqrt{\rho_0/2}e^{i\phi_0}$ where $\rho_0 = \sqrt{\mu/2(U - A)}$ (equivalently $\langle\psi_-\rangle = 0$, $\langle\psi_+\rangle \neq 0$ or $\langle\psi_-\rangle \neq 0$, $\langle\psi_+\rangle = 0$). It is easy to see the symmetry-breaking pattern is described by the coset:

$$U(1)_{\text{soc}} \times U(1)_{ic}/[U(1)_{\text{soc}} \times U(1)_{ic}]_D, \tag{13}$$

where the diagonal (D) means $y \to y + n$, $\phi_0 \to \phi_0 - nk_y^0$ generated by $\mathcal{T}_y^n \times \mathcal{R}(nk_y^0)$ for any integer n. The coset dictates only one Goldstone mode [see Eq. (15)].

Plugging the mean field solution into Eq. (11), one obtain the spin-orbital order of the IC-SkX phase below h_{c2},

$$\langle S_i^+\rangle = \sqrt{\rho_0/2}[u + v + (-1)^{i_x}(u - v)]e^{(-1)^{i_x}i(k_0 i_y + \phi_0)}, \tag{14}$$

where $\langle S_i^z\rangle$ can be fixed by the constraint $|\mathbf{S}_i|^2 = S^2$. It takes the identical form as Eq. (5) after replacing the Bogoliubov transformation matrix elements u, v by the unitary transformation matrix elements c, s. It is remarkable that one can extend the unitary transformation matrix elements c, s in the Z-x phase above h_{c1} and the Bogoliubov transformation matrix elements u, v in the FM state below h_{c2} and reach the same spin-orbital structure of the IC-SkX phase [20]. Well inside the IC-SkX phase, one can identify one exotic gapless Goldstone and one exotic gapped roton mode

$$\begin{aligned}\omega_{+,\mathbf{k}} &= \sqrt{4\rho_0(U - A)\left(v_x^2k_x^2 + v_y^2k_y^2\right)} - V_+\rho_0 k_y,\\ \omega_{-,\mathbf{k}} &= \sqrt{\Delta_-^2 + 8\rho_0 A\left(v_x^2k_x^2 + v_y^2k_y^2\right)} - V_-\rho_0 k_y,\end{aligned} \tag{15}$$

where $\Delta_- = 4\rho_0 A$ is the roton gap, $V_\pm = 4V_1 \pm 2V_2$. One can see that the Goldstone mode achieved from below h_{c2} takes the same form as that in Eq. (6) achieved from above h_{c1}. While the gapped roton mode corresponds to the higher branch $\alpha_{\mathbf{k}}$ in Eq. (2) which is ignored in the effective action Eq. (4). This match is a good check on the consistency between the effective action from h_{c2} down and that from h_{c1} up.

In the following, we study the RG on the two-component QPT near h_{c2} in Fig. 1 and also list the leading operator contents away from the mirror symmetry point. We first derive the RG flow equations at the mirror symmetry point with

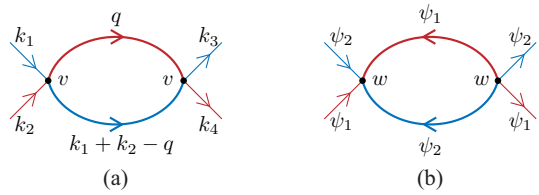

FIG. 3. The renormalization of the mutual interaction v between the two complex order parameters. The same notations as in Fig. 2. (a) Due to v^2, (b) due to w^2.

$w \neq 0$, then setting $w = 0$ to study its RG flow, while putting the RG flow of $w \neq 0$ to the next section.

A. The derivation of the RG flow equations with $w \neq 0$

The effective action describing the magnon BEC in the presence of SOC near $h = h_{c2}$ at the mirror symmetric point $\beta = \pi/4$ in Fig. 1 is

$$\begin{aligned}\mathcal{S}_{\rm MS} = \int d\tau d^d r \sum_{\alpha=1,2} \Big[& \psi^*_\alpha(r,\tau)\partial_\tau \psi_\alpha(r,\tau) \\ & + \frac{\hbar^2}{2m}|\nabla\psi_\alpha(r,\tau)|^2 - \mu|\psi_\alpha(r,\tau)|^2\Big] + \cdots \\ & + u[|\psi_1(r,\tau)|^4 + |\psi_2(r,\tau)|^4] + v|\psi_1(r,\tau)|^2|\psi_2(r,\tau)|^2 \\ & + w[\psi_1(r,\tau)\psi_2(r,\tau)]^2 + w^*[\psi_1^*(r,\tau)\psi_2^*(r,\tau)]^2,\end{aligned} \tag{16}$$

where ψ_1 and ψ_2 are two complex scalar fields. From Eq. (21), one can identify $u = U - A > 0$, $v/2 = U + A > 0$ and $w = B_2$. In fact, w can be made real and its the sign can be changed simply by performing the transformation $\psi_1 \to \psi_1 e^{i\pi/2}$. So the sign of w is irrelevant. Then the three parameters satisfy $A > 2B_2$, namely $v/2 - u > 4w$. After adding back the two type-II dangerously irrelevant operators V_1 and V_2 in Eq. (12), it also describes the QPT near h_{c2} away from the mirror symmetric point in Fig. 1.

The Wilsonian RG equations up to one-loop are shown in Figs. 2–4 and collected as

$$\begin{aligned}\partial_l \mu &= 2\mu, \\ \partial_l u &= \epsilon u - c(u^2 + w^2), \\ \partial_l v &= \epsilon v - c\left(\tfrac{1}{2}v^2 + 8w^2\right), \\ \partial_l w &= \epsilon w - 2c(u+v)w,\end{aligned} \tag{17}$$

where $\epsilon = 2 - d$ and $c = K_d \Lambda^{d-2} 2m/\hbar$ is identical to that in the single-component case Eq. (8). One can see that the

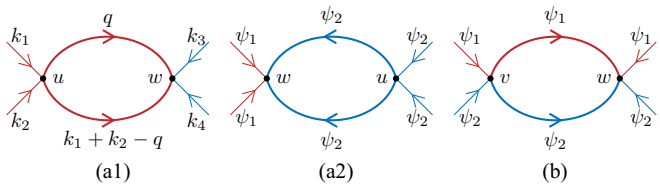

FIG. 4. The renormalization of the umklapp interaction w. The same notations as in Fig. 2. (a1) and (a2) Due to uw, (b) due to vw.

w^2 term renormalizes the u and v, but not itself [24]. As expected, the RG flow remains the same when $w \to -w$. The application to the mirror symmetry case will be presented in Sec. IV.

B. The RG flow pattern and operator contents at $w = 0$

As said in the main text, the w term breaks $U(1)_{ic} \to Z_4$, so $w = 0$ must be a fixed point. If the umklapp term is absent, $w = 0$, then the one-loop RG equations is simplified to

$$\begin{aligned}\partial_l \mu &= 2\mu, \\ \partial_l u &= \epsilon u - cu^2, \\ \partial_l v &= \epsilon v - cv^2/2.\end{aligned} \tag{18}$$

The RG flow of u and v decouples at the one-loop order. At $d = 2$, the RG flow pattern $1/u - 2/v = C$ is given in the $w = 0$ plane of Fig. 6(a). Both are marginally irrelevant at $d = 2$ and lead to new logarithmic violations of scalings to all the physical quantities at a finite T.

In fact, if one rescales v by $1/2$, then v has the same flow equation as u. This is expected, because after setting $w = 0$, the u term is the self-interaction, while the v term is the only the mutual coupling between the two complex fields, so $v = 0$ must be a fixed point also. Naively, one may think Eq. (12) has an enlarged $O(4)$ symmetry at $A = 0$. This is incorrect due to the $z = 2$ term in Eq. (12) which explicitly breaks the $O(4)$ symmetry. If it had been $z = 1$, it would have the enlarged $O(4)$ symmetry at $A = 0$. This is just one aspect of the tremendous differences between $z = 1$ and $z = 2$. In fact, we expect that Eq. (18) is exact to any loop order due to the exact $U(1)_{\rm soc} \times U(1)_{ic}$ symmetry and $z = 2$. Our field theory RG analysis [21] confirms this expectation up to two loops.

In the present case, $u > 0, v > 0$ satisfying $v/2 > u$, so both u and v are type-I marginally irrelevant near h_{c2}, but become relevant above the line of fixed points inside the IC-SkX phase in Fig. 1. It is important to extend Eq. (18) to a finite temperature. Then the two type-I DIOs u and v lead to logarithmic violations of scalings to the two conserved quantities $n_1 = |\psi_1|^2$ and $n_2 = |\psi_2|^2$ (or equivalently $|\psi_1|^2 + |\psi_2|^2$ and $|\psi_1|^2 - |\psi_2|^2$). Then using Eq. (11), one can determine the logarithmic violations of scalings to various quantum spin quantities.

The $v > 0$ means the repulsive interaction between the two species. Imagine the interspecies interaction becomes negative $v < 0$; Eq. (18) shows that it flows to $-\infty$ which indicates the formation of the tightly formed bosonic Cooper pair between ψ_1 and ψ_2.

After adding back the two type-II dangerously irrelevant operators V_1 and V_2 in Eq. (12), just by simple power counting, one finds at $d = 2$

$$\begin{aligned}\partial_l V_1 &= -V_1, \\ \partial_l V_2 &= -V_2,\end{aligned} \tag{19}$$

which are clearly irrelevant near h_{c2}, but change the gapless Goldstone mode and the gapped roton into the exotic form inside the IC-SkX phase. So V_1, V_2 become marginal above the line of fixed points inside the IC-SkX phase in Fig. 1. As shown below Eq. (12), the microscopic calculations find

$V_1, V_2 \sim \sin(2k_0)$ which are indeed exactly marginal along the RG flow in Fig. 1 until hitting the line of fixed points labeled by k_0 inside the IC-SkX phase.

We conclude that away from the mirror symmetry point near h_{c2}, the operator content is two type-I DIOs (u, v) in Eq. (18) and two type-II DIOs (V_1, V_2) in Eq. (19) above the line of stable fixed points inside the IC-SkX (see Fig. 1).

IV. QUANTUM PHASE TRANSITION AT THE UPPER CRITICAL FIELD h_{c2}, THE COMMENSURATE CASE AND MIRROR SYMMETRY POINT

However, if $k_0/\pi = p/q$ where p and q are two co-prime positive integers, then $(\mathcal{T}_y)^{2q} = 1$ and the effective action Eq. (12) should include an extra umklapp term:

$$\mathcal{L}_{\rm um} = B_q(\psi_+\psi_-)^q + \text{c.c.} + iC_q(\psi_+\psi_-)^{q-1}(\psi_+\partial_y\psi_-) + \text{c.c.} + \cdots, \quad (20)$$

where B_q, C_q may be complex for $\beta \neq \pi/4$ and $\cdots$ means high-order terms with power $2nq$ $(n > 1)$. It breaks explicitly only the $U(1)_{ic}$ down to Z_{2q}, but not the $U(1)_{\rm soc}$ symmetry. In the regime $0 \leqslant k_0 \leqslant \pi/2$ in Fig. 1, $q \geqslant 2$, so $\mathcal{L}_{\rm um}$ becomes higher order when $\beta < \pi/4$ with $q > 2$. It becomes highly irrelevant, so can be dropped. All the above results in the IC case also apply to the $q > 2$ C case.

At the mirror symmetry point $\beta = \pi/4$, $k_0 = \pi/2$ with $q = 2$, then $\mathcal{L}_{\rm um}$ is quartic order in $\psi_{1,2}$. So one must consider this B_2 term at $\beta = \pi/4$ where the mirror symmetry dictates $C_2 = 0$ and also the absence of the two type-II DIOs V_1, V_2. Thus,

$$\mathcal{L}_{\rm MS} = \sum_{\alpha=+,-}\left(\psi^*_\alpha\partial_\tau\psi_\alpha + v_x^2|\partial_x\psi_\alpha|^2 + v_y^2|\partial_y\psi_\alpha|^2 - \mu|\psi_\alpha|^2\right) + U(|\psi_+|^2 + |\psi_-|^2)^2 - A(|\psi_+|^2 - |\psi_-|^2)^2 + B_2(\psi_+\psi_-)^2 + \text{c.c.} + \cdots. \quad (21)$$

The microscopic calculations in [15] show $A > 2|B_2|$, so the B_2 term does not change the mean field state. Following the same procedures as those in the IC case, one can extract the excitations as

$$\omega_{+,\mathbf{k}} = \sqrt{4\rho_0(U-A)\left(v_x^2k_x^2 + v_y^2k_y^2\right)},$$
$$\omega_{-,\mathbf{k}} = \sqrt{16\rho_0^2\left(A^2 - 4B_2^2\right) + 8\rho_0 A\left(v_x^2k_x^2 + v_y^2k_y^2\right)}, \quad (22)$$

which recover to the conventional form. It also indicates the umklapp term at $\beta = \pi/4$ does not affect the form of the Goldstone mode, but decreases the roton gap. This is expected, because this B_2 term breaks only the $U(1)_{ic}$ down to Z_4, but not the $U(1)_{\rm soc}$ symmetry.

Now we study the QPT near $h = h_{c2}$. The RG flow equations at one loop were already derived in Eq. (17) where $w = B_2$. $w = 0$ must be a fixed point. This is expected, because the w term breaks $U(1)_{ic} \to Z_4$. Setting $w = 0$ recovers Eq. (18). As to be shown below, in the physically accessible parameter regime $v/2 - u > 4w > 0$, RG flows to the Gaussian fixed point $(u^*, v^*, w^*) = (0, 0, 0)$. So (u, v, w) all lead to new logarithmic violations of scalings to all the physical quantities at a finite T. So there are three type-I DIOs, but no type-II DIOs at the mirror symmetry point near h_{c2}.

Now we study the RG on the two-component QPT near h_{c2} in Fig. 1 and also work out the leading operator contents at the mirror symmetry point. At the mirror symmetry point, one can turn on the w term which breaks $U(1)_{ic} \to Z_4$. At the upper critical dimension $d_u = 2$, $\epsilon = 0$, rescale u, v, w by the positive number c in Eq. (17), i.e., $u \to cu$, $v \to cv$, $w \to cw$; the RG flow equations become

$$\partial_l u = -(u^2 + w^2),$$
$$\partial_l v = -(v^2 + 16w^2)/2, \quad (23)$$
$$\partial_l w = -2(u + v)w,$$

which gives a three-dimensional flow in (u, v, w) space.

For the RG flow Eq. (17) with the three couplings u, v, and w, it would be nice to find an integral motion. Unfortunately, in contrast to the case of the three couplings of fermions near a Fermi surface studied in Ref. [25], we are not able to find any integral motion of the RG flow of Eq. (17). In the following, we find its RG flow pattern first analytically for a small initial value of w_0, then numerically for any initial values of (u_0, v_0, w_0). Finally, we show that with the physically accessible values of (u, v, w), it flows to the Gaussian fixed point $(u_*, v_*, w_*) = (0, 0, 0)$.

A. Analytic perturbation analysis for a small initial w_0

Taking any general initial condition (u_0, v_0, w_0) with $w_0 = 0$, Eq. (18) can be solved analytically:

$$u(l) = \frac{u_0}{1 + u_0 l}, \quad v(l) = \frac{2v_0}{2 + v_0 l}, \quad w(l) = 0. \quad (24)$$

For $|w_0| \ll u_0, v_0$, assume the solution takes the form

$$u(l) = \frac{u_0}{1 + u_0 l} + u_1(l), \quad v(l) = \frac{2v_0}{2 + v_0 l} + v_1(l),$$
$$w(l) = w(l), \quad (25)$$

where $u_1(l), v_1(l), w(l) \to 0$ as $w_0 \to 0$. Ignoring the higher order $[u_1(l)]^2, [v_1(l)]^2$ terms, we reach a new set of differential equations

$$\partial_l u_1 = -\frac{2u_0}{1 + u_0 l}u_1,$$
$$\partial_l v_1 = -\frac{2v_0}{2 + v_0 l}v_1, \quad (26)$$
$$\partial_l w = -2\left(\frac{u_0}{1 + u_0 l} + \frac{2v_0}{2 + v_0 l} + u_1 + v_1\right)w,$$

with initial condition $u_1(0) = 0$, $v_1(0) = 0$, $w(0) = w_0$. The solution is $u_1 = 0$, $v_1 = 0$, and

$$w(l) = \frac{16w_0}{(1 + u_0 l)^2(2 + v_0 l)^4} \sim \frac{16w_0}{u_0^2 v_0^4}\frac{1}{l^4}, \quad (27)$$

where the last $\sim$ shows the asymptotic behavior at a large l. It is clear that with a small w_0 and any positive u_0, v_0, the RG flows to the Gaussian fixed point. In Fig. 5, we plot the differences between the analytical solution and numerical solution, which agree very well in the small-w_0 limit.

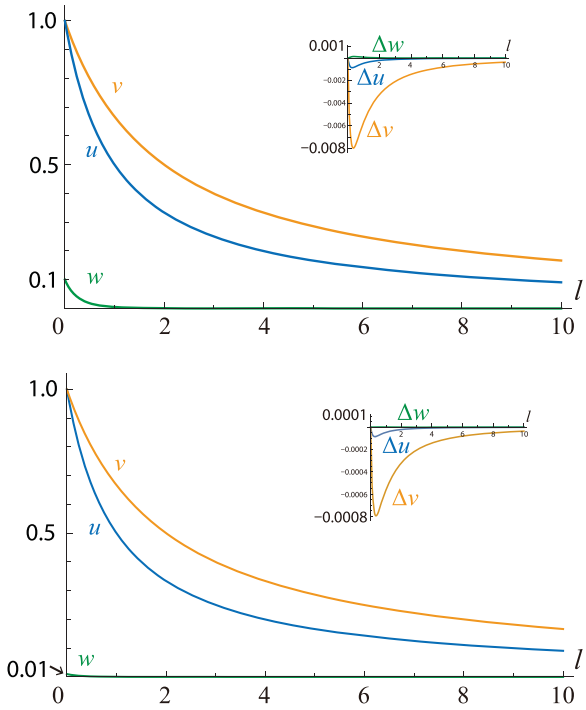

FIG. 5. The solution for RG equations with big initial u_0, v_0, but relatively small initial value w_0. The inset is the differences between the numerical solution and analytical solution Eqs. (25), (27). The top panel is $(u_0, v_0, w_0) = (1, 1, 0.1)$, and the bottom one is $(u_0, v_0, w_0) = (1, 1, 0.01)$. One can see the differences between the numerical solution and analytical solution decrease with $w_0 \to 0$.

B. Numerical solution of the RG flow for any initial values of (u_0, v_0, w_0)

To go beyond the small perturbation presented above, we numerically solve the differential equations (23) for any general initial values of (u_0, v_0, w_0) and highlight the parameter regime which flows to the Gaussian fixed point in Fig. 6(a). Due to the $w \to -w$ symmetry, we only need plot the flows with $w > 0$, and then there is a large stable regime of the Gaussian fixed point inside the first octant.

Then we plot the initial condition wedge $v/2 - u > 4|w|$ and find that it falls within the stability regime in Fig. 6(b). This shows that in the physically allowed parameter regime, the systems flow to the Gaussian fixed point $(u_*, v_*, w_*) = (0, 0, 0)$. All the three operators (u, v, w) are type-I dangerously irrelevant which are marginally irrelevant at the mirror symmetry point in the line of fixed points along h_{c2}, but relevant above the line of fixed points inside the IC-SkX phase (Fig. 1).

It is important to extend Eq. (23) to a finite temperature. Then the three type-I DIOs (u, v, w) lead to logarithmic violations of scalings to one conserved quantity $|\psi_1|^2 + |\psi_2|^2$ and also to $|\psi_1|^2 - |\psi_2|^2$ which is not conserved anymore due to the w term breaking explicitly $U(1)_{ic} \to Z_4$. Then using Eq. (11), one can determine the logarithmic violations of scalings to various quantum spin quantities.

We conclude that at the mirror symmetry point near h_{c2}, the operator content is three type-I DIOs (u, v, w), no type-II DIOs.

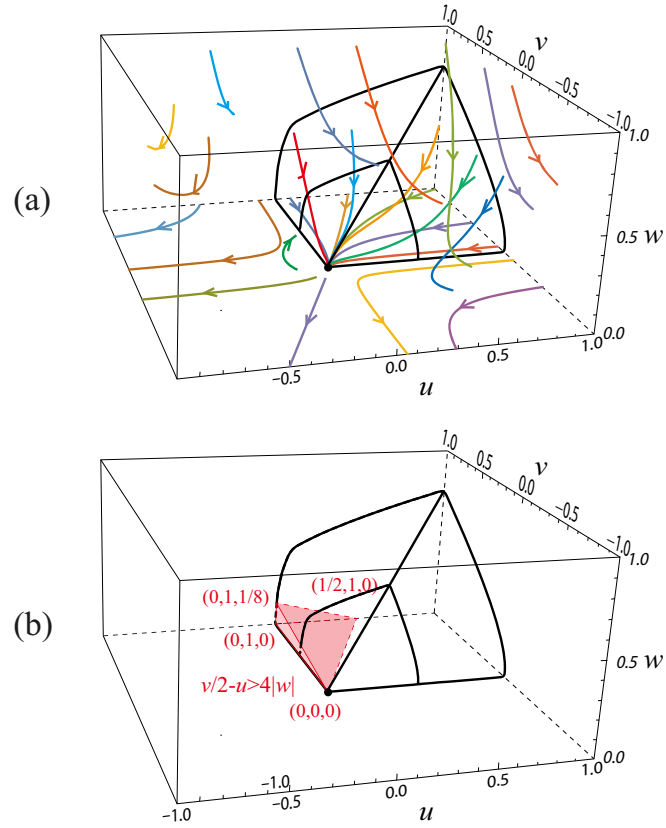

FIG. 6. (a) The renormalization group (RG) flow pattern in the (u, v, w) space. The $w = 0$ plane recovers the RG flow $1/u - 2/v = C$ in Eq. (18), and $C = 0$ gives the straight line flow $1/u = 2/v$. The black thick lines delineate the regime where the RG flows to the Gaussian fixed point. (b) The physically accessible regime (thin red lines) falls inside the stable regime (thick black lines).

V. DISCUSSION AND CONCLUSIONS

In this work, by constructing effective actions from general symmetry principles, contrasting with the previous microscopic calculations well inside a phase and performing RG analysis near the QCPs, we study the BEC of magnons in the presence of SOC which displays many more rich and novel phenomena than those without SOC.

From symmetry analysis, plus some inputs from the microscopic SWE calculations achieved in [14,15], we constructed various effective actions to describe the two transitions driven by the BEC of magnons with the dynamic exponents $z = 2$ at the low and high critical fields. There are one and two type-II dangerously irrelevant operators which lead to exotic excitations inside the IC-SkX phase. (1) The C-IC transition from the Z-x to the IC-SkX at h_{c1}: It has one complex order parameter and one type-II dangerously irrelevant operator. (2) The C-IC transition from the Z-FM to the IC-SkX at h_{c2} in the middle of SOC $\beta_1 < \beta < \beta_2$: It has two complex order parameters with the dynamic exponents $z = 2$ and two type-II dangerously irrelevant operators.

The RG flows, operator contents, and novel line of fixed points labeled by the IC momenta $0 < k_0 < \pi$ in Fig. 1 bring out deep and profound connections between $2 + 1$ dimensional nonrelativistic quantum field theories (QFTs) with $z =$

2 and the nature of the quantum magnets with SOC in a Zeeman field. It remains interesting to construct an F theorem [26] to characterize the RG flow from the UV unstable line of fixed points at h_{c1} or h_{c2} to the stable IR line of fixed points labeled by k_0 inside the IC-SkX phase for such novel QFTs.

As argued in [14], Eq. (1) could be easily realized in recent cold atom experiments [27–31] to generate 2D Rashba SOC for cold atoms on optical lattices in a Zeeman field. The spin-orbital structure of the IC-SkX and its exotic excitations in Fig. 1 can be directly detected by all kinds of Bragg spectroscopy [32–38]. The IC-SkX phase was realized in some materials with a strong Dzyaloshinskii-Moriya (DM) interaction. Indeed, a 2D skyrmion lattice has been observed between $h_{c1} = 50$ mT and $h_{c2} = 70$ mT in some chiral magnets [11] MnSi or a thin film of $Fe_{0.5}Co_{0.5}Si$ [11]. Figure 1 also suggests that the "exotic" intermediate phase observed between $h_{c1} = 7$ T and $h_{c2} = 9$ T in the so-called $4d$ Kitaev material α-$RuCl_3$ [12,13] could be nothing but just the IC-SkX phase discovered here instead of a quantum spin liquid phase. It may also shed some light on the magnon condensation in some dimerized antiferromagnets with SOC [39].

In conventional quantum magnets, as discussed in the Appendix B, the $U(1)_s$ symmetry is only an approximation which can be explicitly broken by many interactions [8–10]. Here, the existence of $U(1)_{\rm soc}$ plays a crucial role in these phenomena which only holds along the $(\alpha = \pi/2, \beta)$ SOC line and the longitudinal Zeeman field. There could also be many ways to break the $U(1)_{\rm soc}$ symmetry explicitly. One way is to apply transverse field. Another is to look at a generic (α, β), or one can apply both at the same time. In [40], we showed that the Z-x state remains stable in a large SOC parameter regime near $\alpha = \pi/2$, and just changes from the exact to the classical ground state. In fact, it is the most robust quantum phase in the whole global phase diagram in the generic (α, β). It would be interesting to look at how Fig. 1, especially the intermediate IC-SkX phase, changes when the $U(1)_{\rm soc}$ symmetry was explicitly broken. It is also important to extend it to the honeycomb lattice where there are three SOC parameters (α, β, γ). It was found that $U(1)_{\rm soc}$ also exists along the anisotropic line $(\alpha = \pi/2, \beta, \gamma = 0)$. Then the results to be achieved in [41] may be directly relevant to the current trends to search for a quantum spin liquid driven by a Zeeman field in $4d$ or $5d$ Kitaev materials.

ACKNOWLEDGMENTS

The authors thank Prof. Gang Tian and Prof. Congjun Wu for the hospitality during their visit at Westlake University. J.Y. thanks Prof. Gang Tian for the hospitality during his visit at the Great Bay University.

APPENDIX A: SPIN-WAVE EXPANSION TO ORDER $1/S$: UNITARY TRANSFORMATION AND BOGOLIUBOV TRANSFORMATION

We first review some results from spin-wave expansion (SWE) performed in [15]. Especially, we stress the unitary transformation in the Z-x state below h_{c1} and the Bogoliubov transformation in the FM state above h_{c2} which are crucial to derive the relations between the quantum spin and the order parameters inside the IC-SkX phase. As presented in Secs. A 1 and A 2, the former is from bottom-up and the latter is from top-down.

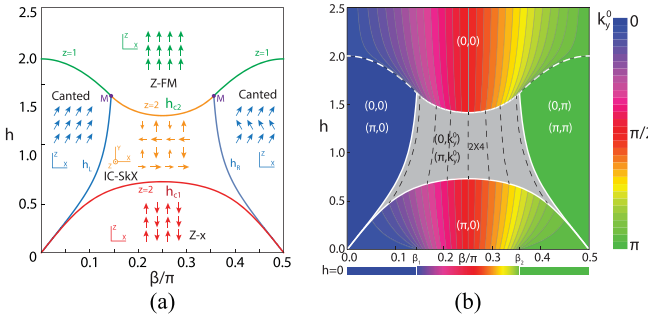

(a) (b)

FIG. 7. (a) Quantum phases and quantum phase transitions of RFHM in a longitudinal Zeeman field Eq. (1) achieved by the microscopic SWE in [15]. The main text focuses on constructing various effective actions and then performing RG analysis on them to study the QPT from the Z-x to the IC-SkX at h_{c1} and from the Z-FM to the IC-SkX at h_{c2} at and away from the mirror symmetry point at $\beta = \pi/4$. There are one and two type-II dangerously irrelevant operators, respectively, which disappear at the mirror symmetry point. (b) The orbital ordering wave vectors of the two collinear, two coplanar, and the noncoplanar phases. The constant contour plot of the minima $(0, k_y^0)$ of the C-IC magnons in the Z-x state at $h < h_{c1}$ and Z-FM state at $h > h_{c2}$, connected by the orbital ordering wave vectors (dashed line) inside the IC-SkX.

1. Unitary transformation in the Z-x state in low field

The spin $S = N/2$ rotated ferromagnetic Heisenberg model at generic SOC parameters (α, β) in a Zeeman field $\vec{H}$ along any direction is [14]

$$\mathcal{H}_{RH} = -J\sum_i [\mathbf{S}_i R(\hat{x}, 2\alpha)\mathbf{S}_{i+\hat{x}} + \mathbf{S}_i R(\hat{y}, 2\beta)\mathbf{S}_{i+\hat{y}}] - \mathbf{H}\cdot\sum_i \mathbf{S}_i, \tag{A1}$$

where the $R(\hat{x}, 2\alpha)$, $R(\hat{y}, 2\beta)$ are two $SO(3)$ rotation matrices around the $\hat{x}, \hat{y}$ spin axis by angle $2\alpha, 2\beta$ putting along the two bonds x, y respectively, and H is the Zeeman field which could be induced by the Raman laser in the cold atom setups.

Following [15], we focus on studying the phenomena along the line $(\alpha = \pi/2, 0 < \beta < \pi/2)$ and in the Zeeman field along the longitudinal y direction. After rotating the spin Y axis to Z axis by the global rotation $R(\hat{x}, \pi/2)$ (or equivalently, one can just put $\beta\sigma_z$ along the y bonds in the square lattice), the Hamiltonian Eq. (A1) along the line $(\alpha = \pi/2, 0 < \beta < \pi/2)$ in the H field along the y direction can be written as Eq. (1). The quantum phase diagram is summarized in Fig. 7.

In a low magnetic field $h < h_{c1}$, the Z-x state is an exact ground state with the classical spin configuration:

$$\mathbf{S}_i = S(0, 0, (-1)^{i_x}), \tag{A2}$$

which breaks the translational symmetry along the x bond to two sites per unit cell (so named as Z-x phase). Thus, one can perform the Holstein-Primakoff transformation for the

sublattice A [15]

$$\begin{aligned} S_i^+ &= \sqrt{2S}\Big(1-\frac{1}{2}\frac{n_i}{2S}+\cdots\Big)a_i,\\ S_i^- &= \sqrt{2S}a_i^\dagger\Big(1-\frac{1}{2}\frac{n_i}{2S}+\cdots\Big),\\ S_i^z &= S-a_i^\dagger a_i, \quad i\in A; \end{aligned} \tag{A3}$$

and for the sublattice B

$$\begin{aligned} S_j^+ &= \sqrt{2S}b_j^\dagger\Big(1-\frac{1}{2}\frac{n_j}{2S}+\cdots\Big),\\ S_j^- &= \sqrt{2S}\Big(1-\frac{1}{2}\frac{n_j}{2S}+\cdots\Big)b_j,\\ S_j^z &= -S+b_j^\dagger b_j, \quad j\in B. \end{aligned} \tag{A4}$$

In momentum space, the Hamiltonian takes the form

$$\begin{aligned} \mathcal{H} =& -2NJS^2+\sum_{\mathbf{k}}[(4JS+H)a_{\mathbf{k}}^\dagger a_{\mathbf{k}}+(4JS-H)b_{\mathbf{k}}^\dagger b_{\mathbf{k}}]\\ &-2JS\sum_{\mathbf{k}}[\cos k_x a_{\mathbf{k}}^\dagger b_{\mathbf{k}}+\cos k_x b_{\mathbf{k}}^\dagger a_{\mathbf{k}}\\ &+\cos(k_y-2\beta)a_{\mathbf{k}}^\dagger a_{\mathbf{k}}+\cos(k_y+2\beta)b_{\mathbf{k}}^\dagger b_{\mathbf{k}}]. \end{aligned} \tag{A5}$$

By performing a unitary transformation

$$a_{\mathbf{k}}=s_{\mathbf{k}}\alpha_{\mathbf{k}}+c_{\mathbf{k}}\beta_{\mathbf{k}}, \quad b_{\mathbf{k}}=s_{\mathbf{k}}\beta_{\mathbf{k}}-c_{\mathbf{k}}\alpha_{\mathbf{k}}, \tag{A6}$$

where $s_{\mathbf{k}}=\sin(\theta_{\mathbf{k},h}/2)$, $c_{\mathbf{k}}=\cos(\theta_{\mathbf{k},h}/2)$ satisfying $c_{\mathbf{k}}^2+s_{\mathbf{k}}^2=1$, and $\tan\theta_{\mathbf{k},h}=\cos k_x/(\sin 2\beta\sin k_y-h)$, the Hamiltonian can be put in the diagonal form:

$$\mathcal{H}=-2NJS^2+4JS\sum_{\mathbf{k}}[\omega_+(\mathbf{k})\alpha_{\mathbf{k}}^\dagger\alpha_{\mathbf{k}}+\omega_-(\mathbf{k})\beta_{\mathbf{k}}^\dagger\beta_{\mathbf{k}}], \tag{A7}$$

where $\mathbf{k}$ is in the reduced Brillouin zone and the excitation spectrum is

$$\begin{aligned} \omega_\pm(\mathbf{k}) =& 1-\tfrac{1}{2}\cos 2\beta\cos k_y\\ &\pm\tfrac{1}{2}\sqrt{\cos^2 k_x+(\sin 2\beta\sin k_y-h)^2}. \end{aligned} \tag{A8}$$

The unitary transformation matrix elements $s_{\mathbf{k}}=\sin(\theta_{\mathbf{k},h}/2)$ and $c_{\mathbf{k}}=\cos(\theta_{\mathbf{k},h}/2)$ are useful to establish the connections between the transverse quantum spin and the order parameter near h_{c1} in Eq. (3).

2. Bogoliubov transformation in the FM in the high field

In a high magnetic field $h>h_{c2}$, the Z-FM state is the classical ground state with the classical spin configuration:

$$\mathbf{S}_i=S(0,0,1). \tag{A9}$$

One can perform the standard Holstein-Primakoff transformation

$$\begin{aligned} S_i^+ &= \sqrt{2S}\Big(1-\frac{1}{2}\frac{n_i}{2S}+\cdots\Big)a_i,\\ S_i^- &= \sqrt{2S}a_i^\dagger\Big(1-\frac{1}{2}\frac{n_i}{2S}+\cdots\Big),\\ S_i^z &= S-a_i^\dagger a_i. \end{aligned} \tag{A10}$$

In momentum space, the Hamiltonian takes the form

$$\begin{aligned} \mathcal{H} =& -NHS+H\sum_{\mathbf{k}}a_{\mathbf{k}}^\dagger a_{\mathbf{k}}-JS\sum_{\mathbf{k}}[2\cos(k_y-2\beta)a_{\mathbf{k}}^\dagger a_{\mathbf{k}}\\ &+\cos k_x(a_{\mathbf{k}}a_{-\mathbf{k}}+a_{\mathbf{k}}^\dagger a_{-\mathbf{k}}^\dagger)]. \end{aligned} \tag{A11}$$

By introducing the Bogoliubov transformation as

$$a_{\mathbf{k}}=u_{\mathbf{k}}\alpha_{\mathbf{k}}+v_{\mathbf{k}}\alpha_{-\mathbf{k}}^\dagger, \quad a_{-\mathbf{k}}^\dagger=v_{\mathbf{k}}\alpha_{\mathbf{k}}+u_{\mathbf{k}}\alpha_{-\mathbf{k}}^\dagger, \tag{A12}$$

where $u_{\mathbf{k}}=\cosh\eta_{\mathbf{k}}$, $v_{\mathbf{k}}=\sinh\eta_{\mathbf{k}}$ satisfying $u_{\mathbf{k}}^2-v_{\mathbf{k}}^2=1$ and $\tanh 2\eta_{\mathbf{k}}=\cos k_x/(h-\cos 2\beta\cos k_y)$, the Hamiltonian takes the diagonal form

$$\begin{aligned} \mathcal{H} &= -NH\Big(S+\frac{1}{2}\Big)+JS\sum_{\mathbf{k}}[\omega(\mathbf{k})\alpha_{\mathbf{k}}^\dagger\alpha_{\mathbf{k}}+\omega(-\mathbf{k})\alpha_{-\mathbf{k}}\alpha_{-\mathbf{k}}^\dagger]\\ &= -NH\Big(S+\frac{1}{2}\Big)+JS\sum_{\mathbf{k}}\omega_{\mathbf{k}}+2JS\sum_{\mathbf{k}}\omega_{\mathbf{k}}\alpha_{\mathbf{k}}^\dagger\alpha_{\mathbf{k}}, \end{aligned} \tag{A13}$$

where $\mathbf{k}$ is in the Brillouin zone and the spin wave dispersion is

$$\omega_{\mathbf{k}}=\sqrt{(h-\cos 2\beta\cos k_y)^2-\cos^2 k_x}-\sin 2\beta\sin k_y. \tag{A14}$$

The Bogoliubov transformation matrix elements $u_{\mathbf{k}}$ and $v_{\mathbf{k}}$ are useful to establish the connections between the transverse quantum spin and the order parameter near h_{c2} in Eq. (11).

APPENDIX B: THE BEC OF MAGNONS OF AN AFM IN A UNIFORM FIELD: THE $U(1)_s$ CASE

An AFM Heisenberg model in a uniform field breaks the spin $SU(2)_s$ to the spin $U(1)_s$. A high $h>h_c$ leads to a fully polarized state, the Z-FM state, which is not only the ground state but also an exact eigenstate. A simple spin-wave calculation shows $\omega\sim\Delta+v^2k^2$ near (π,π) which is nothing but a gapped FM mode; the order parameter is simply a complex field ψ. Because the Z-FM is the exact ground state which does not break the translational symmetry, neither the Bogoliubov transformation nor unitary transformation is needed, and thus the relation between the quantum spin in a square lattice and the order parameter in a continuum is simply

$$\langle S_i^+\rangle=(-1)^{i_x+i_y}\psi, \tag{B1}$$

which is much simpler than Eq. (3) and (11) for the $U(1)_{\rm soc}$ case. Of course, this mapping only works near the QCP $h\sim h_c$, and will break down near $h\sim 0$.

The effective action consistent with the $U(1)_s$ symmetry and the translational symmetries is

$$\mathcal{L}_{U(1)_s}=\psi^*\partial_\tau\psi+v^2|\nabla\psi|^2-\mu|\psi|^2+U|\psi|^4+\cdots, \tag{B2}$$

where $\mu=h-h_c$. It belongs to $z=2$ zero density SF-Mott transition universality class, and therefore confirms the assumption used in [7].

When $\mu<0$, $\langle\psi\rangle=0$ the mean field ground state is the Z-FM state (Fig. 8).

When $\mu>0$, $\langle\psi\rangle=me^{i\phi_0}$ where $m=\sqrt{\mu/2U}$, the mean field ground state is $\mathbf{S}_i=((-1)^{i_x+i_y}m\cos\phi_0,(-1)^{i_x+i_y}m\sin\phi_0,\sqrt{S^2-m})$, which is

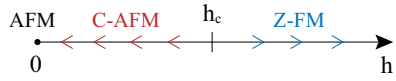

FIG. 8. Quantum phase transitions of an AFM in a Zeeman field. C-AFM means the canted coplanar AFM state, Z-FM means the FM along the Zeeman field direction. There is only one critical field h_c, no intermediate phase. The arrows indicate the RG flow, and there is only one unstable (QPT) fixed point at h_c. It is constructive to compare with the mirror symmetry line with $\beta = \pi/4$ in Fig. 7(a) and RG flow in Fig. 1.

the canted co-planar AFM state (Fig. 8). It supports one gapless Goldstone mode $\omega_k = ck$ due to the $U(1)_s$ symmetry breaking.

As stressed in the main text, U in Eq. (B2) is the well known type-I dangerously irrelevant operator. In fact, it is also marginally irrelevant at the upper critical dimension $d = 2$, but it is crucial to determine the symmetry-breaking ground state and leads to the violation of the hyperscaling at or above the upper critical dimension.

When comparing with Eq. (4), one can see it is identical to Eq. (4) near $h = h_{c1}$ at the mirror symmetric point $\beta = \pi/4$. However, due to the dramatic difference between the Eq. (B1) and Eq. (3) which express the *very different* quantum spin order in terms of the *identical* order parameter, in the resulting symmetry-breaking state the canted AFM in the former is completely different than the IC-SkX in the latter, but the Goldstone mode still takes the same form. However, away from the mirror symmetric point $\beta \neq \pi/4$, the DIO V term in Eq. (4) moves in which does not touch the ground state, but changes its excitation to the exotic form Eq. (6).

Furthermore, in the SOC case studied in the main text, there are two critical fields h_{c1}, h_{c2} and an intermediate phase IC-SkX between the two critical ones. The Z-FM when $h > h_{c1}$ is just a classical ground state instead of an exact ground state, so it supports strong quantum fluctuations, in sharp contrast to the Z-FM in Eq. (B1) which is an exact ground state with no quantum fluctuations. Here without the SOC, there is only one h_c which is very similar to h_{c1} at the mirror symmetric point $\beta = \pi/4$, and no intermediate phase (Fig. 8). These dramatic differences demonstrate the new features of the SOC in magnetic systems.

[1] F. London, On the Bose-Einstein condensation, Phys. Rev. **54**, 947 (1938).

[2] M. H. Anderson, J. R. Ensher, M. R. Matthews, C. E. Wieman, and E. A. Cornell, Observation of Bose-Einstein condensation in a dilute atomic vapor, Science **269**, 198 (1995).

[3] K. B. Davis, M. O. Mewes, M. R. Andrews, N. J. van Druten, D. S. Durfee, D. M. Kurn, and W. Ketterle, Bose-Einstein Condensation in a Gas of Sodium Atoms, Phys. Rev. Lett. **75**, 3969 (1995).

[4] T. Nikuni, M. Oshikawa, A. Oosawa, and H. Tanaka, Bose-Einstein Condensation of Dilute Magnons in $TlCuCl_3$, Phys. Rev. Lett. **84**, 5868 (2000).

[5] T. Radu, H. Wilhelm, V. Yushankhai, D. Kovrizhin, R. Coldea, Z. Tylczynski, T. Lühmann, and F. Steglich, Bose-Einstein Condensation of Magnons in Cs_2CuCl_4, Phys. Rev. Lett. **95**, 127202 (2005).

[6] V. E. Demidov, O. Dzyapko, S. O. Demokritov, G. A. Melkov, and A. N. Slavin, Observation of Spontaneous Coherence in Bose-Einstein Condensate of Magnons, Phys. Rev. Lett. **100**, 047205 (2008).

[7] S. Sachdev, T. Senthil, and R. Shankar, Finite-temperature properties of quantum antiferromagnets in a uniform magnetic field in one and two dimensions, Phys. Rev. B **50**, 258 (1994).

[8] For a review, see C. Lhuillier and G. Misguich, in *High Magnetic Fields*, Lecture Notes in Physics, Vol. 595, edited by C. Berthier, L. P. Lévy, and G. Martinez (Springer, Berlin, Heidelberg, 2002), pp. 161–190.

[9] S. Sachdev, *Quantum Phase Transitions*, 2nd ed. (Cambridge University Press, Cambridge, 2011).

[10] V. Zapf, M. Jaime, and C. D. Batista, Bose-Einstein condensation in quantum magnets, Rev. Mod. Phys. **86**, 563 (2014); **86**, 1453(E) (2014).

[11] X. Z. Yu, Y. Onose, N. Kanazawa, J. H. Park, J. H. Han, Y. Matsui, N. Nagaosa, and Y. Tokura, Real-space observation of a two-dimensional skyrmion crystal, Nature (London) **465**, 901 (2010).

[12] Y. Kasahara, T. Ohnishi, and Y. Mizukami, O. Tanaka, Sixiao Ma, K. Sugii, N. Kurita, H. Tanaka, J. Nasu, Y. Motome, T. Shibauchi, and Y. Matsuda, Majorana quantization and half-integer thermal quantum Hall effect in a Kitaev spin liquid, Nature (London) **559**, 227 (2018).

[13] Y. Kasahara, K. Sugii, T. Ohnishi, M. Shimozawa, M. Yamashita, N. Kurita, H. Tanaka, J. Nasu, Y. Motome, T. Shibauchi, and Y. Matsuda, Unusual Thermal Hall Effect in a Kitaev Spin Liquid Candidate α-$RuCl_3$, Phys. Rev. Lett. **120**, 217205 (2018).

[14] F. Sun, J. Ye, and W.-M. Liu, Quantum magnetism of spinor bosons in optical lattices with synthetic non-Abelian gauge fields at zero and finite temperatures, Phys. Rev. A **92**, 043609 (2015).

[15] F. Sun, J. Ye, and W.-M. Liu, Quantum incommensurate skyrmion crystals and commensurate to incommensurate transitions in cold atoms and materials with spin-orbit couplings in a Zeeman field, New J. Phys. **19**, 083015 (2017).

[16] A. V. Chubukov, S. Sachdev, and J. Ye, Theory of two-dimensional quantum Heisenberg antiferromagnets with a nearly critical ground state, Phys. Rev. B **49**, 11919 (1994).

[17] In a classical or quantum phase transition, a dangerously irrelevant operator is irrelevant near the transition, but determines the nature of the symmetry-breaking ground state. We name the known one [7,9,16] as type I. Here, we identify a new type of dangerously irrelevant operator which is irrelevant near a QPT, does not change the ground state in the symmetry breaking phase, but changes its excitation spectrum to an exotic form. We name the new one type II dangerously irrelevant operator (DIO). In terms of danger, the type II is weaker than type I.

[18] In Eq. (1), the S^+S^+ and S^-S^- terms belong to the Kitaev-like (compass) term. The third term consists of the term $\cos 2\beta(S_i^+S_{i+y}^- + S_i^-S_{i+y}^+)$ which belongs to the Heisenberg interaction, and also the term $i\sin 2\beta(S_i^+S_{i+y}^- - S_i^-S_{i+y}^+)$ which belongs to the Dzyaloshinskii-Moriya (DM) interaction. This is due to the fact that Eq. (1) contains the Heisenberg, Kitaev (or compass), and DM interaction as stressed in [14].

[19] Due to the factoring of $e^{ik_0 i_y}$ in Eq. (3) and in Eq. (11), the odd derivative in the ∂_y term first appears in the interaction V term and V_1, V_2 terms, respectively.

[20] Its symmetry-breaking pattern and associated Goldstone mode are identical to Eq. (13).

[21] J. Ye, Coulomb interaction at superconductor to Mott insulator transition, Phys. Rev. B **58**, 9450 (1998).

[22] Despite that the universality class is completely determined by the order parameter ψ, due to the relation Eq. (5) between the quantum spin on the lattice and the order parameter ψ in the effective action, the two states are very much different than those in the SF-Mott transition. The boson BEC leads to a superfluid, while the magnon BEC leads to a quantum magnetic order.

[23] Here we only focus on the the middle range $\beta_1 < \beta < \beta_2$ in Fig. 1.

[24] Here u and v are two type-II DIOs, and should not be confused with the Bogoliubov transformation coefficients u and v in Eq. (11).

[25] J. Ye and S. Sachdev, Superconducting, metallic, and insulating phases in a model of CuO_2 layers, Phys. Rev. B **44**, 10173 (1991).

[26] T. Nishioka, Entanglement entropy: Holography and renormalization group, Rev. Mod. Phys. **90**, 035007 (2018).

[27] L. Huang, Z. Meng, P. Wang, P. Peng, S.-L. Zhang, L. Chen, D. Li, Q. Zhou, and J. Zhang, Experimental realization of a two-dimensional synthetic spin-orbit coupling in ultracold Fermi gases, Nat. Phys. **12**, 540 (2016).

[28] Z. Meng, L. Huang, P. Peng, D. Li, L. Chen, Y. Xu, C. Zhang, P. Wang, and J. Zhang, Experimental Observation of Topological Band Gap Opening in Ultracold Fermi Gases with Two-Dimensional Spin-Orbit Coupling, Phys. Rev. Lett. **117**, 235304 (2016).

[29] M. L. Wall, A. P. Koller, S. Li, X. Zhang, N. R. Cooper, J. Ye, and A. M. Rey, Synthetic Spin-Orbit Coupling in an Optical Lattice Clock, Phys. Rev. Lett. **116**, 035301 (2016).

[30] Z. Wu, L. Zhang, W. Sun, X.-T. Xu, B.-Z. Wang, S.-C. Ji, Y. Deng, S. Chen, X.-J. Liu, and J.-W. Pan, Realization of two-dimensional spin-orbit coupling for Bose-Einstein condensates, Science **354**, 83 (2016).

[31] N. Q. Burdick, Y. Tang, and B. L. Lev, Long-Lived Spin-Orbit-Coupled Degenerate Dipolar Fermi Gas, Phys. Rev. X **6**, 031022 (2016).

[32] J. Ye, J. M. Zhang, W. M. Liu, K. Zhang, Y. Li, and W. Zhang Light-scattering detection of quantum phases of ultracold atoms in optical lattices, Phys. Rev. A **83**, 051604(R) (2011).

[33] J. Ye, K. Y. Zhang, Y. Li, Y. Chen, and W. P. Zhang, Optical Bragg, atom Bragg and cavity QED detections of quantum phases and excitation spectra of ultracold atoms in bipartite and frustrated optical lattices, Ann. Phys. **328**, 103 (2013).

[34] M. Kozuma, L. Deng, E. W. Hagley, J. Wen, R. Lutwak, K. Helmerson, S. L. Rolston, and W. D. Phillips, Coherent Splitting of Bose-Einstein Condensed Atoms with Optically Induced Bragg Diffraction, Phys. Rev. Lett. **82**, 871 (1999).

[35] J. Stenger, S. Inouye, A. P. Chikkatur, D. M. Stamper-Kurn, D. E. Pritchard, and W. Ketterle, Bragg Spectroscopy of a Bose-Einstein Condensate, Phys. Rev. Lett. **82**, 4569 (1999).

[36] D. M. Stamper-Kurn, A. P. Chikkatur, A. Görlitz, S. Inouye, S. Gupta, D. E. Pritchard, and W. Ketterle, Excitation of Phonons in a Bose-Einstein Condensate by Light Scattering, Phys. Rev. Lett. **83**, 2876 (1999).

[37] J. Steinhauer, R. Ozeri, N. Katz, and N. Davidson, Excitation Spectrum of a Bose-Einstein Condensate, Phys. Rev. Lett. **88**, 120407 (2002).

[38] S. B. Papp, J. M. Pino, R. J. Wild, S. Ronen, C. E. Wieman, D. S. Jin, and E. A. Cornell, Bragg Spectroscopy of a Strongly Interacting ^{85}Rb Bose-Einstein Condensate, Phys. Rev. Lett. **101**, 135301 (2008).

[39] Q.-R. Zhao, M.-J. Sun, Z.-X. Liu, and J. Wang, Magnon condensation in dimerized antiferromagnets with spin-orbit coupling, Phys. Rev. B **105**, 094401 (2022).

[40] F. Sun and J. Ye, Complete, incomplete devil staircases and Luttinger liquids Cantor set of strongly interacting spin-orbit coupled bosons in a lattice, arXiv:1603.00451.

[41] F. Sun and J. Ye (unpublished).